Computation of Nonlinear One-Dimensional Waves in Near-Sonic Flows

A. H. Nayfeh,* B. S. Shaker,† and J. E. Kaiser‡
Virginia Polytechnic Institute and State University, Blacksburg, Va.

A nonlinear analysis is developed for sound propagation in a variable-area duct in which the mean flow approaches choking conditions. A quasi-one dimensional model is used; results of the standard linear theory are compared with the nonlinear results to assess the significance of the nonlinear terms. The nonlinear analysis represents the acoustic disturbance as a sum of interacting harmonics. Numerical results show that the basic signal is unaffected by the presence of higher harmonics if the throat Mach number is not too large, but as the Mach number approaches unity, more harmonics are needed to describe the acoustic propagation. The strong interactions among harmonics in the numerical results occur in a region which is generally consistent with the nonlinear inner-expansion region of Myers and Callegari, i.e., the interaction occurs when $\delta^{1/2}/(1-|M|)=0(1)$, where δ is the amplitude of the acoustic disturbance. In addition, the results indicate that complete analysis of strong nonlinear interactions will require modeling of acoustic shocks.

I. Introduction

ALTHOUGH choked inlets have been recognized as an effective means of reducing upstream noise propagation,[1,2] the physical mechanisms that are responsible for the noise reduction are not well understood. In particular, no analytical technique that is capable of providing a proper model of sound propagation through partially choked inlets or that is capable of explaining some differences among several experimental results has been developed to date.

It has been well established that the linear acoustic theory is not valid as the mean-flow Mach number approaches unity.[3-6] However, attempts to incorporate nonlinear effects into a study of sound propagation through a near-sonic mean-flow region are in the developmental stage. One such attempt[4] treats the nonlinear terms as a source disturbance to the basic linear propagation process. Such an approach cannot succeed, since it does not remove the mathematical singularity from the differential operator in the governing physical equations. Another analysis[5] uses matched asymptotic expansions to examine the region where $1-|M|=0(\epsilon)$. Explicit confirmation of the singular behavior of the linear theory is obtained, and from matching considerations the nonlinear effects are inferred to be important when the strength of the acoustic disturbance is the order of $(1-|M|)^2$, but no linear results are reported.

This paper describes the status of an investigation into nonlinear acoustic propagation through compressible mean flows that appraoch sonic conditions. To gain insight into the mechanisms that operate in the near-sonic region and to determine the mathematical techniques required to analyze these mechanisms, we have examined the behavior of numerical solutions of the nonlinear, one-dimensional equations of motion. The one-dimensional model contains all the essential elements of the linear singularity and of the nonlinear harmonic interactions without the purely computational difficulties of the full two-dimensional problem. The acoustic disturbance is represented as a sum of a basic frequency and a finite number of higher harmonics, and the nonlinear interaction among the harmonics and their complex conjugates are calculated.

The wave-envelope technique of an earlier study[6] of linear acoustic propagation, in which the linear acoustic disturbance is represented as a superposition of quasiparallel duct modes whose fast axial variation is explicitly given, is not used because of the singular behavior of the linear model in the region of interest. The singular behavior of the linear model as the Mach number approaches unity is illustrated in Fig. 1. The abrupt rise in amplitude of the acoustic disturbance is indicative of a need to include nonlinear terms. However, direct comparisons of nonlinear and linear results reported herein show that, in many cases, the linear results remain valid to Mach numbers higher than would be expected on the basis of a cursory inspection of results such as those shown in Fig. 1. Thus, a linear model that can handle the effects of large axial gradients, such as the wave-envelope technique, can be applied over most of the flowfield in a converging-diverging duct, and the region to be bridged by the nonlinear analysis is small in many cases.

The development of the equations that describe the interactions among the harmonics and the numerical solution of these equations is described in Sec. II, the results are com-

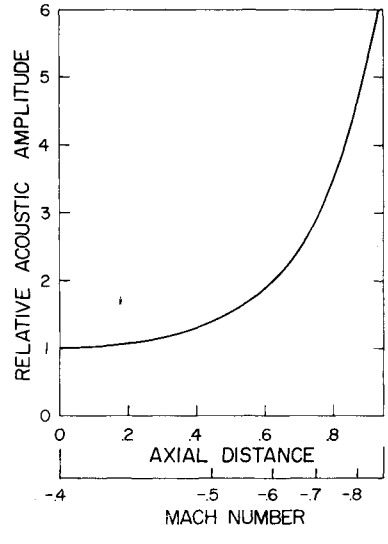

Fig. 1 Increase of linear acoustic amplitude with mean flow Mach number $\omega=1$.

Presented as Paper 77-1297 at the AIAA 4th Aeroacoustics Conference, Atlanta, Ga., Oct. 3-5, 1977; submitted Oct. 28, 1977; revision received July 27, 1978.

Index categories: Noise; Powerplant Design.

*University Distinguished Professor of Engineering. Member AIAA.

†Presently, Assistant Professor, King Abdulaziz University, Jeddah, Saudi Arabia.

‡Associate Professor, Dept. of Engineering Science & Mechanics. Member AIAA.

pared with known exact solutions for uniform ducts in Sec. III, and numerical results for variable-area ducts are given in Sec. IV.

II. Problem Formulation and Method of Solution

We consider a one-dimensional, inviscid, nonlinear flow in a hard-walled duct (Fig. 2). All flow quantities are expressed in nondimensional form using the speed of sound c_a evaluated at some convenient point as a reference velocity, the radius R_0 of the duct in the uniform region as the reference length, and R_0/c_a, $\rho_a c_a^2$, ρ_a, and T_a as the reference time, pressure, density, and temperature, respectively. The one-dimensional equations of motion are:

Mass

$$A\frac{\partial \rho}{\partial t}+\frac{\partial}{\partial x}(\rho u A)=0 \tag{1}$$

where A is the cross-sectional area of the duct.

Momentum

$$\rho\left[\frac{\partial u}{\partial t}+u\frac{\partial u}{\partial x}\right]+\frac{\partial p}{\partial x}=0 \tag{2}$$

Energy

$$\rho\left[\frac{\partial T}{\partial t}+u\frac{\partial T}{\partial x}\right]-(\gamma-1)\left[\frac{\partial p}{\partial t}+u\frac{\partial p}{\partial x}\right]=0 \tag{3}$$

State

$$\gamma p=\rho T \tag{4}$$

where γ is the ratio of specific heats of the gas. The energy and state equations, Eqs. (3) and (4), can be replaced with the isentropic state equations $p\propto\rho^{\gamma}$. However, the use of this apparently simpler equation would lead to difficulties in separating the effects of the several harmonics in the analysis which follows; therefore, the basic forms of the energy and state equations are used.

The flow variables are represented as the sum of a steady mean-flow part plus the acoustic disturbances:

$$u(x,t)=u_0(x)+u_{10}+\sum_{n=1}^{N}\left(u_{1_n}e^{-in\omega t}+\bar{u}_{1_n}e^{in\omega t}\right) \tag{5}$$

$$\rho(x,t)=\rho_0(x)+\rho_{10}+\sum_{n=1}^{N}\left(\rho_{1_n}e^{-in\omega t}+\bar{\rho}_{1_n}e^{in\omega t}\right) \tag{6}$$

$$T(x,t)=T_0(x)+T_{10}+\sum_{n=1}^{N}\left(T_{1_n}e^{-in\omega t}+\bar{T}_{1_n}e^{in\omega t}\right) \tag{7}$$

with the pressure being eliminated with Eq. (4). The mean-flow terms, denoted by $(\,)_0$, are solutions of the steady form of Eqs. (1-4). With the area expressed as a function of axial distance and the Mach number in the straight-duct section given, all mean-flow values are easily obtained from the standard one-dimensional gasdynamic equations:

$$\frac{A(x)}{A(0)}=\frac{M(0)}{M(x)}\left[\frac{1+\frac{\gamma-1}{2}M^2(x)}{1+\frac{\gamma+1}{2}M^2(0)}\right]^{\frac{\gamma+1}{2(\gamma-1)}} \tag{8}$$

$$\frac{T_0(x)}{T_0(0)}=\frac{1+\frac{\gamma-1}{2}M^2(0)}{1+\frac{\gamma-1}{2}M^2(x)} \tag{9}$$

etc.

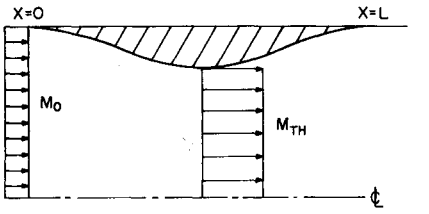

Fig. 2 Duct geometry.

Reference conditions are chosen to be the mean-flow quantities in the straight-duct section so that $T_0(0)=\rho_0(0)=1$, $u_0(0)=M(0)$, and $p_0(0)=1/\gamma$. The acoustic disturbance in Eqs. (5-7) is represented as a finite sum of harmonics, including steady streaming terms u_{10}, etc., and the complex conjugates must be explicitly stated since nonlinear interactions are considered.

No assumption about the axial variation of the acoustic quantities is made. Although the wavelengths of upstream propagating signals become small and thus a technique similar to the wave-envelope procedure would be very advantageous, no a priori assumption about that variation can be made. No assumptions about the relative sizes of the terms in Eqs. (5-7) are made, except that the steady streaming terms are small compared with the mean-flow terms. If these terms are not small, the mean flow cannot be uncoupled from the acoustic disturbance; that is, the mean flow is not given by Eqs. (8) and (9) but must be solved simultaneously with the acoustic disturbance without separation of the mean flow and the steady streaming.

Substituting the expansion of the flow variables, Eqs. (5-7), into the governing equations, (1-4), subtracting the equations governing the mean flow, and equating the coefficients of equal power of $\exp(in\omega t)$ for $n=1,2\ldots$ to zero, one obtains a set of coupled, nonlinear ordinary differential equations of the form

$$A(x,y)\frac{dy}{dx}=B(x,y) \tag{10}$$

where y is a column vector of the unknowns. The coefficient matrix $A(x,y)$ and the inhomogeneous vector $B(x,y)$ are given in the Appendix.

We choose to solve Eq. (10) in the real form. To accomplish this we rewrite Eq. (10) as

$$(A_r+iA_i)\left(\frac{dy_r}{dx}+i\frac{dy_i}{dx}\right)=(B_r+iB_i) \tag{11}$$

Separation of the real and imaginary parts leads to

$$A_r\frac{dy_r}{dx}-A_i\frac{dy_i}{dx}=B_r \tag{12}$$

$$A_i\frac{dy_r}{dx}+A_r\frac{dy_i}{dx}=B_i \tag{13}$$

Since the steady streaming is always real, its imaginary part in Eqs. (12) and (13) is discarded. This manipulation reduces Eq. (10) to

$$A^*(x,y^*)\frac{dy^*}{dx}=B^*(x,y^*) \tag{14}$$

where A^* is a $3(2N+1)\times 3(2N+1)$ real matrix and y^* and B^* are $3(2N+1)$ column vectors.

Numerical Solution

Equation (14) can be solved by a forward-integration technique if one inverts the matrix A^* at each axial step. For

this study, we have employed a fourth-order Runge-Kutta routine. Since the dimension of the matrix A^* increases proportionally to the number of harmonics included, the computation time increases rapidly with the number of harmonics. Numerical results have shown that few harmonics are needed to obtain accurate results for the fundamental frequency.

One disadvantage of this direct approach can be identified immediately. The terms of the coefficient matrix A^* are often small, especially those derived from the energy and mass equations; thus, as the number of harmonics increases the determinant of the matrix becomes smaller. A reformulation of the problem in terms of an integrability constraint, similar to the approach used in the wave-envelope study,[6] which would avoid this difficulty, is now under consideration.

The initial conditions at the duct entrance are specified in terms of a reflection coefficient. Conditions in the straight-duct section are assumed to be such that linear theory is adequate. Thus the acoustic signal at the duct entrance is resolved into left- and right-running waves. The magnitude of the input signal (right-running wave) and the value of the reflection coefficient (which determines the left-running wave) are specified as input at $x=0$, and the program integrates through the duct to determine the corresponding conditions at $x=L$. Determination of the transmission and reflection characteristics of the duct section then would require an iteration on the assumed value of the reflection coefficient until the desired zero input conditions at $x=L$ are achieved. Such an iteration on the input conditions is essential in the nonlinear case; furthermore, these transmission and reflection characteristics will be a function of the strength of the input signal. A central-difference procedure to solve Eq. (14) would allow a direct imposition of the appropriate end conditions, but would require an iteration on the nonlinear terms of Eq. (14). The central-difference method has not been programmed for this study, but a detailed evaluation of the efficiencies of the two numerical procedures should be made at a future date.

III. Comparison with Exact Solutions

The propagation of a finite-amplitude acoustic wave in a uniform, lossless medium can be described by the implicit, exact solution of Earnshaw.[7] This solution is valid in a straight, rigid duct provided one neglects the small attenuation and dispersion produced by the walls. For a sinusoidal source disturbance, Fubini[8] has expanded the Earnshaw solution into an explicit representation of the development of each harmonic part of the acoustic signal; this solution remains valid up to the point of shock formation. Blackstock[9] has extended the Fubini solution into the region where a shock develops and the signal decays to the standard N-wave pattern. Each of these results was derived for a wave propagating in a medium at rest, but they are easily applied to propagation through a uniform mean flow by analyzing the problem for the moving medium by employing either a coordinate transformation[10] or the method of renormalization, the method of multiple scales, etc.[11,12]

The Fubini solution expresses the acoustic disturbance that results from a sinusoidal source disturbance of frequency ω and strength δ in the form

$$u_1(x,t)=\delta\sum_{n=1}^{\infty}B_n\sin n(\omega t-kx) \tag{15}$$

$$B_n=(2\ell/nx)J_n(nx/\ell) \tag{16}$$

where J_n is the Bessel function of the first kind of order n and ℓ is the distance to shock formation, which, including the effect of the mean flow, is

$$\ell=\frac{2(1+M)^2}{\delta\omega(\gamma+1)} \tag{17}$$

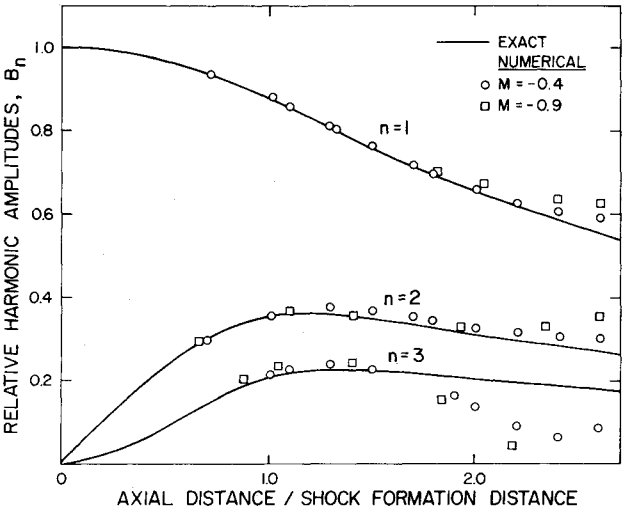

Fig. 3 Development of harmonic amplitudes in a straight duct $\omega=1$, $\rho_1=0.013$.

Note that the harmonic amplitudes are independent of the mean-flow Mach number if considered to be functions of x/ℓ. These results are valid only up to the point of shock formation. The development of the harmonic amplitudes, including the effect of a discontinuous shock, is given by the Blackstock solution[9]

$$B_n=\frac{2}{n\pi}\sin\Phi_{\min}+\frac{2\ell}{n\pi x}\int_{\Phi_{\min}}^{\pi}\cos n(\Phi-\frac{x}{\ell}\sin\Phi)d\Phi \tag{18}$$

where

$$\Phi_{\min}=(x/\ell)\sin\Phi_{\min}$$

Φ is the phase angle of the initial sinusoidal disturbance, and $\Phi_{\min}$ locates the portion of the wave that has been absorbed into the shock. If $x/\ell<1$, then $\Phi_{\min}=0$ and evaluation of the integral in Eq. (18) leads to the Fubini solution, Eq. (16). This exact result has been calculated and compared with numerical results from the method described in Sec. II applied to a straight duct. For comparison of the results, the numerical procedure imposes a zero value of the reflection coefficient at $x=0$ and imposes an initial amplitude of zero on all harmonics except u_{11}. Furthermore, the following relations between the exact solution and the numerical procedure are used:

$$\delta=2\,|u_{11}(0)|$$

$$B_n=|u_{1_n}|/|u_{11}(0)|$$

The comparison of the results is shown in Fig. 3. The numerical results were calculated with four harmonics for several values of the mean-flow Mach number. Up to shock formation the results agree very well for all values of the Mach number; at distances beyond shock formation the numerical results do not agree exactly with the analytic results, but at least for the fundamental signal the results show the proper trend and are not grossly in error. Since the numerical calculations are based on an inviscid model, the agreement is better than one would anticipate and probably is aided by an artificial viscosity induced by the numerical procedure. The main conclusions to be noted from these results are that the occurrence of shocks in the acoustic disturbance creates no catastrophic problems for the numerical procedure and the nonlinear effects as $|M|\to 1$ contain no transonic effects beyond the cumulative distortion of the signal that is present in the Fubini and Blackstock solutions. Highly accurate results from the numerical

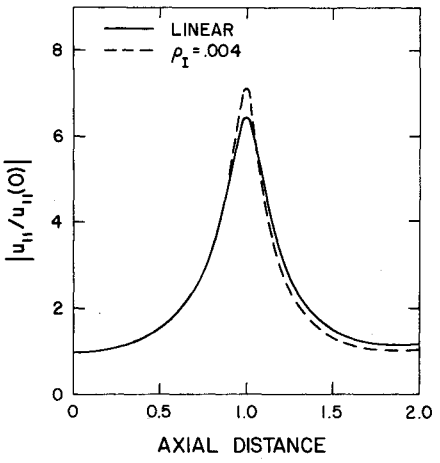

Fig. 4 Comparison of linear and nonlinear results for the fundamental frequency for increasing strengths of the acoustic input, $\omega = 1$, $M_0 = -0.40$, $M_{TH} = -0.86$, reflection coefficient = 0, $N = 2$.

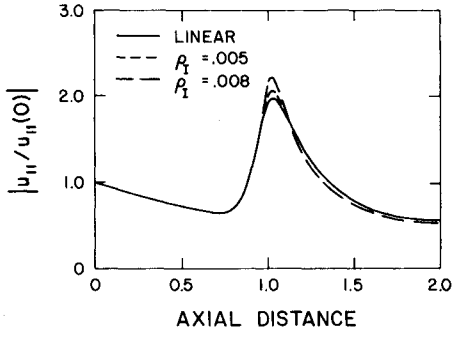

Fig. 5 Comparison of linear and nonlinear results for the fundamental frequency for increasing strengths of the acoustic input, $\omega = 1$, $M_0 = +0.40$, $M_{TH} = +0.86$, reflection coefficient $= -0.34 - 0.93i$, $N = 2$.

procedure in the shock development region, especially for the higher harmonics, will require the inclusion of viscous effects.

IV. Variable-Area Results

The numerical procedure has been applied to examine acoustic propagation through a simple converging-diverging duct section. The radius of the duct wall in the variable-area section is given by

$$R = 1 - a_2[1 - \cos(2\pi x/L)]$$

and the duct connects to straight sections at $x = 0$ and $x = L$ (see Fig. 2).

The program has been used to obtain solutions to both the nonlinear and linear forms of the basic equations in order to assess the basic importance of the nonlinear terms under various flow conditions. Two types of initial conditions at $x = 0$ are considered: the simplest is an arbitrary specification of a zero value of the reflection coefficient; the other case specifies the value of the reflection coefficient to be the value determined by linear theory. Since the results and general conclusions were the same for these cases, iteration on the nonlinear equations to find the exact value of the reflection coefficient was not considered necessary at this stage.

Figure 4 illustrates the effect of increasing the strength of the input signal (ρ_I is the density disturbance at $x = 0$) for a case in which the mean-flow Mach number varies from -0.40 at $x = 0$ to -0.86 at the throat, and only the right-running wave is present at $x = 0$. Figure 5 has the same effect except that the mean flow is from left to right ($M > 0$) and an upstream wave at $x = 0$ occurs only as a consequence of reflection of a downstream input signal. Both cases show

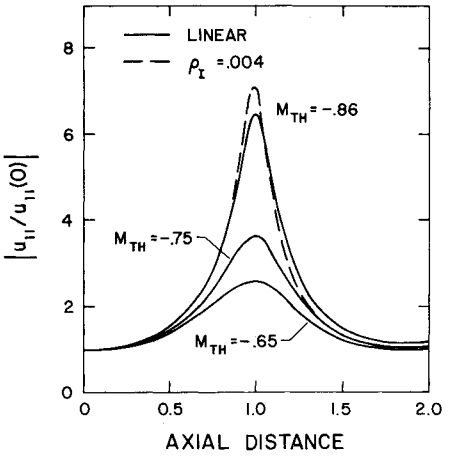

Fig. 6 Comparison of linear and nonlinear results for the fundamental frequency for increasing values of the mean flow Mach number, $\omega = 1$, reflection coefficient = 0, $N = 2$.

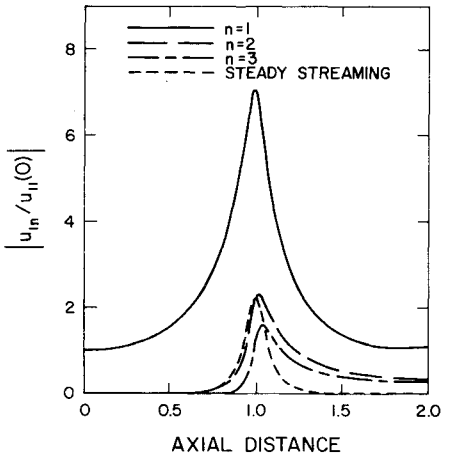

Fig. 7 Development of harmonic amplitudes and steady-streaming amplitude, $\omega = 1$, $M_0 = -0.4$, $M_{TH} = -0.86$, $\rho_I = 0.004$, reflection coefficient = 0, $N = 4$.

essentially the same trends, with the effects being more pronounced for the case in which the upstream wave is dominant. For small values of the input signal, the nonlinear and linear results coincide as expected. As ρ_I is increased, the effect of the nonlinearity is to increase the intensity of the disturbance near the throat region. The increased intensity results in a transfer of energy to the higher harmonics; thus, the fundamental signal has a lower amplitude at the exit due to the nonlinearity. Figure 6 shows the effects of increasing the mean-flow Mach number with the strength of the input signal fixed. At the lower values of the throat Mach number, the nonlinear results do not differ from the linear results. As the throat Mach number increases, the same trends occur as noted earlier—an intensification of the disturbance in the throat region occurs along with a corresponding decrease at the exit. The results in Figs. 4-6 were obtained by calculating only two harmonics (plus the steady streaming term); however, an increase to four harmonics yields the same results for the fundamental signal. One can also note that the linear results in these cases break down only very close to the throat region.

The behavior of the higher harmonics is illustrated in Fig. 7. The higher harmonics reach peaks near the throat and decrease to nonzero values at the exit. Thus a net shift from the fundamental signal to the higher harmonics occurs. The steady streaming is important in the throat region but decreases to insignificant values at the exit. Although the steady streaming is significant relative to the acoustic

disturbance, we note that the maximum values of the steady streaming terms in all the calculations presented in this paper are less than 1% of the mean-flow terms. Thus, uncoupling the mean flow from the steady streaming and acoustic disturbances, as in Eq. (5), is justifiable.

The development of significant nonlinear effects in the cases depicted in Figs. 4-7 is consistent with the criterion proposed by Myers and Callegari[5] that $\delta^{1/2} = 0(1 - |M|)$. In the numerical results, nonlinear effects become important when $\delta^{1/2}/(1 - |M|)$ is approximately 0.8, if one uses the local values at the throat to evaluate the expression. However, it should be noted that the parameter $(1+M)^2/\delta$ is proportional to the distance to shock formation of a sinusoidal signal; i.e., from Eq. (17)

$$\ell = \frac{2}{\gamma+1}\frac{(1+M)^2}{\delta\omega}$$

Thus, in those cases in which nonlinear effects become large, it appears that an inviscid model is not adequate and the influence of viscosity will be important.

The cases illustrated in Figs. 4-7 are for weak or moderate nonlinear effects. If the strength of the input signal and/or the throat Mach number is increased, the numerical procedure eventually produces either a strong oscillation or abrupt jumps in the acoustic signal near the duct throat. The origin of these instabilities has been investigated in some detail. Refinement of the numerical step size produces no qualitative change in the instabilities. Moreover, an increase in the number of harmonics does not cure the problem. In fact, cases have been calculated in which a doubling of the number of harmonics causes a discontinuity or instabililty to develop. Calculation of the acoustic waveform from the harmonic amplitudes has indicated that acoustic shocks are developing in these cases of strong nonlinear interaction; however, the results of the straight duct indicate that the presence of these shocks should not cause such instabilities. In addition, the steady-streaming terms are increasing to significant proportions relative to the mean flow. Preliminary calculations in which the mean flow and acoustic disturbance are coupled have been made; this procedure does not remove the instabilities, but the results demonstrate that the acoustic disturbance does have a significant influence on the mean flow in these cases of strong nonlinear interaction. These preliminary calculations indicate that the acoustic disturbance increases rather than decreases the mean flow; that is, there is an energy transfer from the acoustic disturbance to the mean flow and not vice versa. Viscous terms were added to the acoustic equations in the form of sink terms as well as in a finite-difference form. Neither of these approaches solved the problem.

Checking the determinant of the coefficient matrix A, we found that in every instability case the determinant approaches zero at an axial position which depends on the Mach number, the strength and frequency of the input signal, and the number of harmonics. If the mesh size is sufficiently coarse, the calculations may proceed through the duct without developing an apparent instability. However, refining the step size would show the instability. We note that the results in Figs. 4-7 were checked by decreasing the step size and no instabililties were observed. Based on the preceding discussion, we conclude that, in the cases where the determinant approaches zero, the right-hand side of Eq. (14) must be orthogonal to every solution of its adjoint homogeneous problem in order to remove the singularity and hence the instability. This condition will determine the proper values of the reflection coefficients at the initial location. Hence, an iterative scheme needs to be introduced to enable the satisfaction of this orthogonality condition. Thus, the physics of the flow near the throat dictates the amount of reflection and this may be the mechanism which reduces the noise in partially choked inlets. Moreover, the amount of reduction depends on the values of the reflection coefficients which in turn depends on the mean flow Mach number and the strength and frequency content of the noise.

V. Conclusions and Recommendations

A numerical procedure for analysis of nonlinear acoustic propagation through high subsonic mean flows has been developed. The numerical results show that the nonlinearity intensifies the acoustic disturbance in the throat region, leading to a shift of energy to the higher harmonics and a reduction of the intensity of the fundamental frequency at the duct exit. The numerical procedure calculates cases of moderate nonlinear interaction satisfactorily but develops an instability for cases of strong interaction. For high-input signals and/or throat Mach numbers, the steady-streaming terms may not be negligible relative to the mean flow; thus the mean flow needs to be coupled with the acoustic disturbance. In addition, the numerical results show that acoustic shocks are developing as a result of the strong nonlinear interactions. Thus, a complete analysis of this problem has to include coupling of the mean flow with the acoustic disturbance and perhaps viscous effects near the shocks. Most important, an iterative scheme should be introduced to satisfy an orthogonality condition and hence determine the values of the reflection coefficients.

Appendix

If y is the column vector of the unknowns $\tilde{u}_{1N},\ldots,u_{1N},\tilde{\rho}_{1N},\ldots,\tilde{\rho}_{1N},\tilde{T}_{1N},\ldots T_{1N}$ the coefficient of Eq. (10) take the following forms:

$$A(x,y) = \begin{bmatrix} \alpha_{11} & \alpha_{12} & \alpha_{13} \\ \alpha_{21} & \alpha_{22} & \alpha_{23} \\ \alpha_{31} & \alpha_{32} & \alpha_{33} \end{bmatrix}$$

where α_{ij} are $(2N+1)\times(2N\times 1)$ submatricies defined as:

$$\alpha_{nm} = \begin{bmatrix} E_{nm}(0) & \tilde{E}_{nm}(1) & \tilde{E}_{nm}(2) & \cdots \\ E_{nm}(1) & E_{nm}(0) & \tilde{E}_{nm}(1) & \cdots \\ E_{nm}(2) & E_{nm}(1) & E_{nm}(0) & \cdots \\ \vdots & \vdots & \vdots & \end{bmatrix}$$

where

$$E_{11}(0) = \rho_0 + \rho_{10}, \quad E_{12}(0) = u_0 + u_{10}, \quad E_{13}(0) = 0$$

$$E_{11}(n) = \rho_{1_n}, \quad E_{12}(n) = u_{1_n}, \quad E_{13}(n) = 0$$

$$E_{21}(0) = \rho_0 u_0 + \rho_0 u_{10} + u_0 \rho_{10} + F_1(0), \quad E_{22}(0) = \frac{T_0 + T_{10}}{\gamma}, \quad E_{23}(0) = \frac{\rho_0 + \rho_{10}}{\gamma}$$

$$E_{21}(n) = \rho_0 u_{1_n} + u_0 \rho_{1_n} + F_1(n), \quad E_{22}(n) = \frac{T_{1n}}{\gamma}, \quad E_{23}(n) = \frac{\rho_{1n}}{\gamma}$$

$$E_{31}(0)=0, \quad E_{32}(0)=(1-\gamma)[T_0u_0+T_0u_{10}+u_0T_{10}+F_2(0)] \quad E_{33}(0)=E_{21}(0)$$

$$E_{31}(n)=0, \quad E_{32}(n)=(1-\gamma)(T_0u_{1_n}+u_0T_{1_n}+F_2(n)), \qquad E_{33}(n)=E_{21}(n)$$

$$F_1(0)=\sum_{j=-N}^{N} u_{1_j}\bar{\rho}_{1_j}, \text{ where } (\,)_{1,-n}\equiv(\bar{\ })_{1,n}, \quad F_1(1)=\sum_{j=-N}^{N-1}\bar{\rho}_{1_j}u_{1_{j+1}}, \quad F_1(2)=\rho_{11}u_{11}+\sum_{j=-N}^{N-2}\bar{\rho}_{1_j}u_{1_{j+2}}$$

etc.

$F_2(n)$ has the same form as $F_1(n)$ but with ρ being replaced by T.

$$B=\begin{bmatrix} B_1(n) \\ B_2(n) \\ B_3(n) \end{bmatrix} \qquad n=-N,\ldots,0,\ldots,N$$

where

$$B_1(n)=-[in\omega\rho_{1_n}+c_1u_{1_n}+\rho_{1_n}c_2+F_1(n)A_s]$$

$$B_2(n)=-\left[in\rho_0\omega u_{1_n}+a_1\rho_{1_n}+a_2u_{1_n}+a_3T_{1_n}+F_1(n)\frac{\partial u_0}{\partial x}+F_5(n)\right]$$

$$B_3(n)=-\left[F_3(n)+(1-\gamma)F_4(n)+i\omega n\rho_0T_{1_n}+i(1-\gamma)\times n\omega T_0\rho_{1_n}+F_1(n)\frac{\partial T_0}{\partial x}+(1-\gamma)F_2(n)\frac{\partial \rho_0}{\partial x}+a_4u_{1_n}+a_5\rho_{1_n}+a_6T_{1_n}\right]$$

$$a_1=u_0\frac{\partial u_0}{\partial x}+\frac{1}{\gamma}\frac{\partial T_0}{\partial x}, \quad a_2=\rho_0\frac{\partial u_0}{\partial x}, \quad a_3=\frac{1}{\gamma}\frac{\partial \rho_0}{\partial x}$$

$$a_4=\rho_0\frac{\partial T_0}{\partial x}+(1-\gamma)T_0\frac{\partial \rho_0}{\partial x}, \quad a_5=u_0\frac{\partial T_0}{\partial x}$$

$$a_6=(1-\gamma)u_0\frac{\partial \rho_0}{\partial x}, \quad c_1=\frac{\partial \rho_0}{\partial x}+\rho_0A_s, \quad c_2=\frac{\partial u_0}{\partial x}+u_0A_s$$

$$A_s=\frac{1}{A}\frac{\mathrm{d}A}{\mathrm{d}x}$$

$$F_3(0)=\sum_{j=-N}^{N}\bar{\rho}_{1_j}i\omega_jT_{1_j}$$

$$F_3(1)=\sum_{j=-N}^{N-1}\bar{\rho}_{1_j}i\omega(j+1)T_{1_{j+1}}$$

etc.

:

$F_4(n)$ has the same form as $F_3(n)$ but with ρ, T being replaced by T, ρ, respectively.

$F_5(n)$ has the same form as $F_3(n)$ with T being replaced by u.

Acknowledgment

This work was perfomed under support from the NASA Langley Research Center, Contract No. NAS1-13884.

References

[1] Greatrex, F. B., "By-Pass Engine Noise," *SAE Transactions*, Vol. 69, 1961, pp. 312-324.

[2] Sobel, J. A. and Welliver, A. D., "Sonic Block Silencing for Axial and Screw-Type Compressors," *Noise Control*, Vol. 7, No. 5, Sept./Oct. 1961, pp. 9-11.

[3] Eisenberg, N. A. and Kao, T. W., "Propagation of Sound Through a Variable-Area Duct with a Steady Compressible Flow," *Journal of Acoustical Society of America*, Vol. 49, Jan. 1971, pp. 169-175.

[4] Hersh, A. S. and Liu, C. Y., "Sound Propagation in Choked Ducts," CR-135123, NASA, 1976.

[5] Myers, M. K. and Callegari, A. J., "On the Singular Behavior of Linear Acoustic Theory in Near-Sonic Duct Flows," *Journal of Sound and Vibration*, Vol. 51, April 1977, pp. 517-531.

[6] Nayfeh, A. H., Shaker, B. S., and Kaiser, J. E., "Transmission of Sound Through Nonuniform Circular Ducts with Compressible Mean Flows," CR-145126, NASA, May 1977.

[7] Earnshaw, S., "On the Mathematical Theory of Sound," *Philosophical Transactions of the Royal Society, London*, Vol. 150, 1860, pp. 133-148.

[8] Fubini, E., "Anomalie Nella Propagazione di onle Acustische die Grande Ampiezza," *Alta Frequenza*, Vol. 4, 1935, pp. 530-581.

[9] Blackstock, D. T., "Connection between the Fay and Fubini Solution for a Plane Sound Wave of Finite Amplitude," *The Journal of the Acoustical Society of America*, Vol. 39, June 1966, pp. 1019-1026.

[10] Polyakova, A. L., "Plane Sound Waves of Finite Amplitude in a Moving Medium," *Soviet Physics-Doklody*, Vol. 6, 1961, pp. 344-345.

[11] Nayfeh, A. H. and Kaiser, J. E., "Nonlinear Propagation of Arbitrary Plane Waves in Ducts Carrying Plug Flows," AIAA Paper 75-846, Hartford, Conn., June 1975.

[12] Nayfeh, A. H. and Kluwick, A., "A Comparison of Three Perturbation Methods for Nonlinear Hyperbolic Waves," *Journal of Sound and Vibration*, Vol. 48, No. 2, Sept. 1976, pp. 293-299.